Human kallikrein 6 inhibitors with a *para*-amidobenzylanmine P1 group identified through virtual screening

Guyan Liang [a,*], Xin Chen [a,*,†], Suzanne Aldous [b], Su-Fen Pu [c], Shujaath Mehdi [d], Elaine Powers [e], Tianhui Xia [f,‡], Rachel Wang [f]

[a] Molecular Innovative Therapeutics, Sanofi Pharmaceuticals, Bridgewater, NJ, USA
[b] Fibrosis and Wound Repair, Sanofi Pharmaceuticals, Bridgewater, NJ, USA
[c] Global Pharmacovigilance & Epidemiology, Sanofi Pharmaceuticals, Bridgewater, NJ, USA
[d] Immunology and Inflammation Unit, Sanofi Pharmaceuticals, Bridgewater, NJ, USA
[e] Early to Candidate Unit, Sanofi Pharmaceuticals, Bridgewater, NJ, USA
[f] Biotherapeutics, Sanofi Pharmaceuticals, Bridgewater, NJ, USA

ARTICLE INFO

ABSTRACT

A series of hK6 inhibitors with a *para*-amidobenzylamine P1 group and a 2-hydroxybenzamide scaffold linker was discovered through virtual screening. The X-ray structure of hK6 complexed with compound **9b** was determined to a resolution of 1.68 Å. The tertiary folding of the hK6 complexed with the inhibitor is conserved relative to the structure of the apo-protein, whereas the interaction between hK6 and the inhibitor is consistent with both the SAR and the *in silico* model used in the virtual screening.

© 2012 Elsevier Ltd. All rights reserved.

Human tissue kallikreins (hKs), also referred to as KLKs for their genes, are trypsin-like serine proteases belonging to family S1A in Clan PA(S) according to MEROPS classification.[1–4] With 15 members identified so far, hKs 1–15, human tissue kallikreins have played an important role in various physiological processes. The first human tissue kallikrein (hK1) was originally identified in 1920s from pancreas and was believed to be able to regulate blood pressure by releasing lysyl-bradykinin (kallidin) from kininogen, in a mechanism similar to the one for human plasma kallikrein.[5] hK2 and hK3, more notably known as prostate specific antigen (PSA), have been broadly used as biomarkers for prostate cancer. Similar functions have been postulated for other hKs, such as hKs 3/6 for breast cancer, and hKs 6/9/10/11 for ovarian cancer.[6–13]

In addition to its role as a diagnostic biomarker for various cancers, it has been suggested that hK6 is a potential therapeutic tar-

get for neurodegenerative diseases, such as Alzheimer's disease and multiple sclerosis (MS).[14–17] On concentration heat maps generated from reverse transcription PCR studies, hK6 exhibited elevated expression in CNS.[16] Clinical evidence of hK6 accumulation in human brain lesions and in vivo studies in mice suggested that hK6 promoted MS progression by causing CNS inflammation and neuron demyelination.[18–20] The involvement of hK6 in demyelination was demonstrated by Scarisbrick and co-workers to be connected to its enzymatic activity, for example, its ability to degrade myelin-associated proteins, such as rat myelin basic protein (MBP) and rat myelin oligodendrocyte glycoprotein (αMOG).[18] Therefore, inhibitors that can regulate hK6 enzymatic function are of significant pharmaceutical interest. The present article describes the discovery of hK6 inhibitors with a *para*-amidobenzylamine scaffold, which can be further developed as therapeutic agents.

While an enormous amount of research has been done for design, synthesis, and characterization of other trypsin-like serine proteases, such as fXa, fVIIa, thrombin, elastase, and tryptase, publications on kallikrein inhibitors, however, have been scarce. Kallikrein inhibitors published so far are mostly limited to mechanism-based and/or peptidic inhibitors. Accounting for about 10% of human plasma, serpins are the most abundant endogenous kallikrein inhibitors,

---

for example, serpin α1-antitrypsin (ATT) for hK7, serpin α1-chymorypsin (ACT) and serpin antithrombin (AT) for hK6, and serpin α2-antiplasmin (AP) for hKs 2/4/5/12.[21–23] Serpins are mechanism-based macromolecular inhibitors that can form a covalent bond with the catalytic serine residue of hKs and render them enzymatically inactive.

Exogenous inhibitors described in the literature have also been mostly limited to mechanism-based and peptide-like molecules, such as leupeptin, antipain, the soybean trypsin inhibitor (SBTI), the lima bean trypsin inhibitor (LBTI), and the bovine pancreatic trypsin inhibitor (BPTI), which all form a covalent bond with serine 195 of the catalytic triad. The contribution of the covalent bond to the overall binding affinity overshadows the non-bonded interaction of the rest of the molecule, thus mechanism-based inhibitors, especially irreversible ones, are often challenged for their lack of selectivity against other serine proteases and their risk of long-term toxicity associated with the poor selectivity.[24–28] Furthermore, many of those inhibitors are polypeptidic macromolecules, for which it is extremely challenging, if not impossible, to achieve orally bioavailability.

While some non-mechanism-based small organic inhibitors have been published for other kallikreins, to our knowledge, none has been reported for hK6 that are suitable for pharmaceutical development. In the 1970s, Geratz and co-workers discovered a series of diamidino inhibitors for hK1, then referred to as pancreatic kallikrein, such as compounds **1** and **2** in Figure 1.[29–32] In 2000, Okada et al. reported plasma kallikrein inhibitors with aminomethylcyclohexyl moiety as a P1 group, compound **3** in Figure 1.[33] In 2001, a series of hK3 inhibitors with azetidinone scaffold, such as compound **4** in Figure 1, was reported by Adlington et al.[34] In 2006, scientists from Celera disclosed a groups of plasma kallikrein inhibitors with a 5-amidinobenzimidazole P1 group, among which the most potent one has a K_i of 0.5 nM, compound **5** Figure 1.[35] In 2008, LeBeau's group published their finding of peptidic boronic acid inhibitors for hK3 with the best K_i of 65 nM, such as compound **6** in Figure 1. X-ray structures exhibited that the boronic acid of the inhibitor interacted with the catalytic serine and the lysine side chain of the inhibitor bound in the S1 pocket.[36,37] Research for hK6 inhibitors, especially those suitable for pharmaceutical development, is rather primitive. For example, although benzamidine and *para*-aminobenzamidine were identified in the S1 pocket of hKs 1, 4, and 6 through X-ray crystallography, their potency was rather weak (20% hK6 inhibition at 63 μM for benzamidine).[38,39]

Based on the X-ray structure determined and made publically available by Bernett and co-workers, the tertiary folding of hK6 is highly similar to other trypsin-like serine proteases. Figure 2 shows the structure of hK6 superimposed with several representative trypsin-like serine proteases including fVIIa, fXa, thrombin, trypsin, and β-tryptase with only alpha carbon trace visible. As shown in the figure, while some loops further away from the substrate-binding site deviate from one other, the backbone folding of the group based on alpha carbon atoms at the binding site is highly conserved. This conserved folding offers an opportunity for inhibitors of other trypsin-like serine proteases to bind with hK6.

The side-chain tertiary folding for hK6 is also conserved in general except one significant insertion at the position of Ile218/Pro219. As shown in Figure 3, while the Pro219 faces away from the substrate-binding site, the Ile218 side-chain shifts towards the catalytic center. Even if this moderate change does not interfere with the substrate binding, it cannot be tolerated by some typical inhibitors of trypsin-like serine proteases. For example, Otamixaban, an fXa inhibitor well-advanced in clinical study, has a steric collision with Ile218 if it remains in its native fXa binding mode, as shown in Figure 4 (top). Similarly, the binding of a β-tryptase inhibitor with a benzylamine P1 and piperidineamide scaffold linker in its native mode is also blocked by Ile218, Figure 4 (bottom). For both examples, molecular dynamics (MD) simulations indicated that the mobility of the inhibitor is too limited to accommodate the intrusion of Ile218 and Pro219. Additionally, according to both X-ray structures and MD simulations, the conformation of Ile218 and Pro219 did not exhibit much flexibility to mitigate the steric collision either.

Two sets of compounds were selected through *in silico* virtual screening. The first set covered compounds that bound well in the hK6 binding site without shifting away from their native binding modes in the original serine protease where the compound showed its highest potency. The second set included compounds that could not bind in hK6 in their native binding mode, but were able to adopt a new binding mode in hK6 without significant energy penalty in docking. While more compounds were selected from the first set, representatives for each scaffold in the second set were also included for enzymatic testing. The resulting screening set was further filtered to remove known mechanism-based protease inhibitors and compounds with reactive functional groups.

For our investigation, the same hK6 construct was used for both enzymatic testing and crystallography. The cDNA of mature hK6 was cloned into pBAC-3 vector with an N-terminus His6-tag and
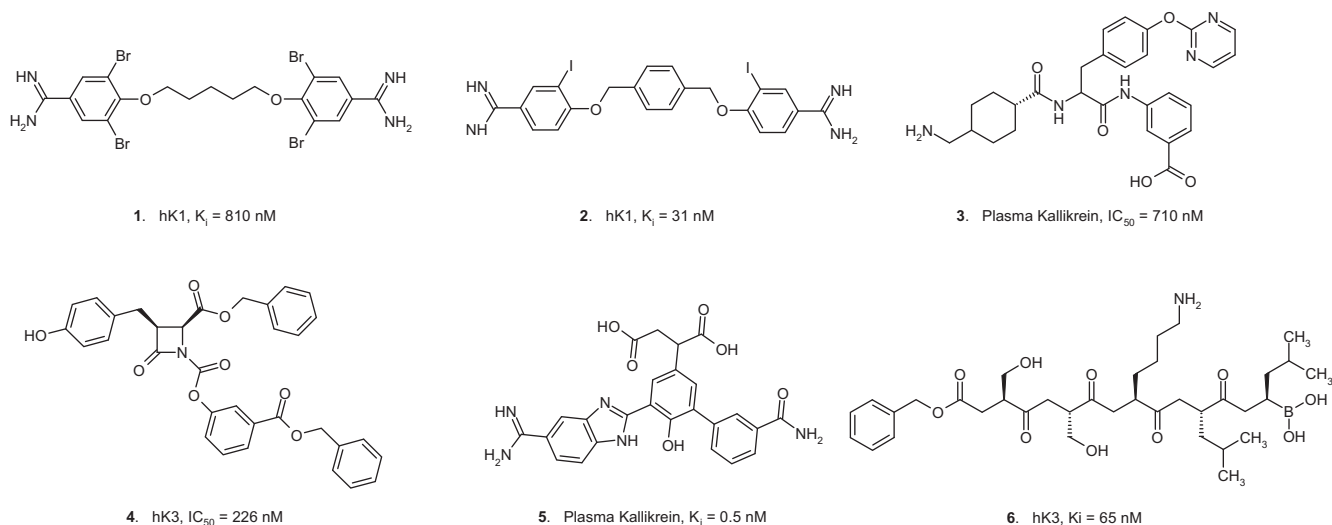

1. hK1, K_i = 810 nM

2. hK1, K_i = 31 nM

3. Plasma Kallikrein, IC$_{50}$ = 710 nM

4. hK3, IC$_{50}$ = 226 nM

5. Plasma Kallikrein, K_i = 0.5 nM

6. hK3, Ki = 65 nM

Figure 1. Representative small organic kallikrein inhibitors.
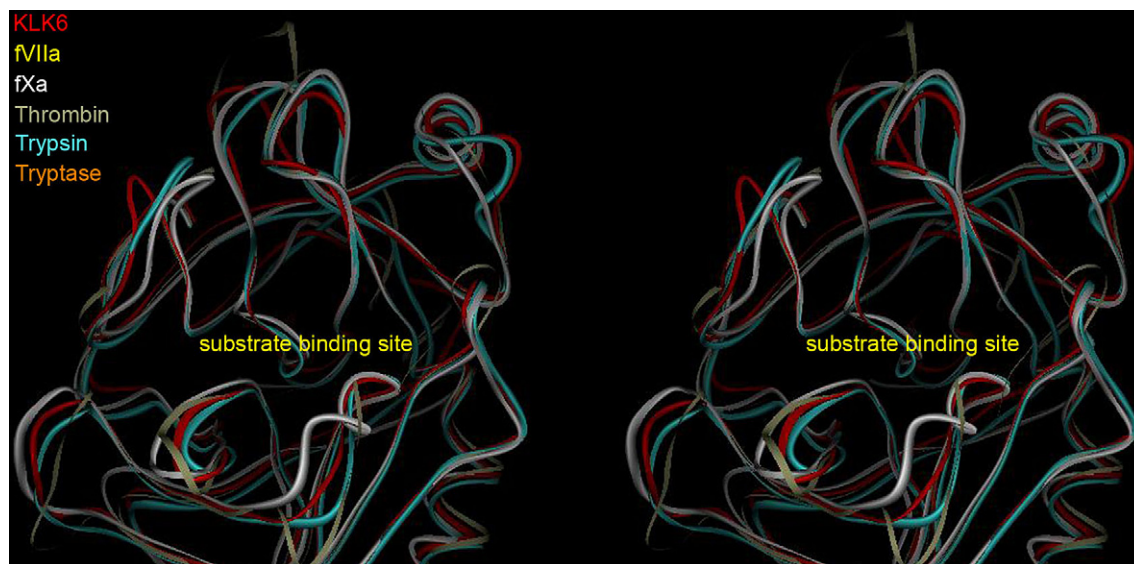
Figure 2. Stereo view of representative trypsin-like serine proteases superimposed on substrate-binding pocket with only alpha-carbon trace shown.
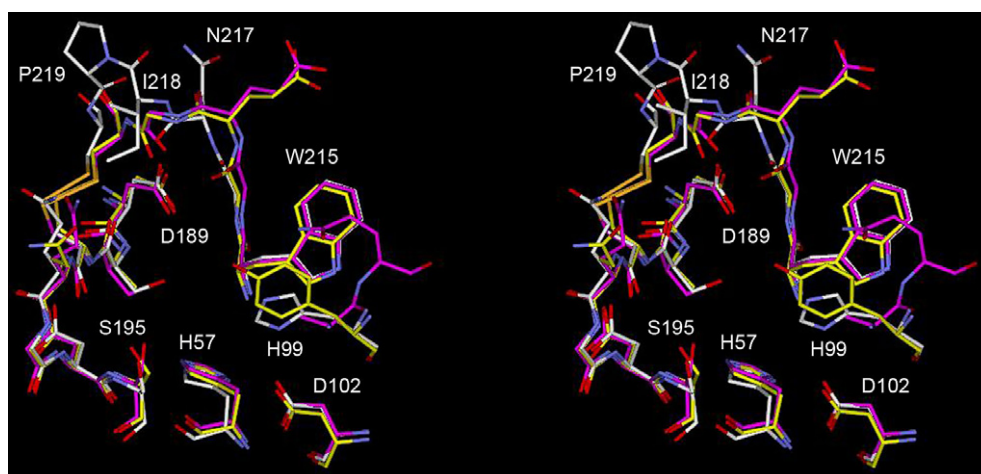

Figure 3. Stereo view of the substrate-binding site of hK6 superimposed with fXa and β-tryptase. Carbon atoms of hK6 are colored in white, while those for fXa and β-tryptase are colored in yellow and magenta, respectively.

an enterokinase (EK) cleavage sequence, (Asp)$_4$Lys. A Baculovirus/ Sf9 cell line was used with essentially the same process as the one described by Blaber et al.[20] Three mutations (R74G, R76Q and N132Q) were introduced to prevent autolysis and glycosylation. The protein was purified with Ni-NTA column followed by activation with EK (EK light chain, New England Biolabs® P8070L) in an EK to hK6 ratio of 1:10,000.

Compounds selected by virtual screening were tested in the same activation buffer solution in black 96-well plates at room temperature using the substrate of tBoc-Phe-Ser-Arg-AMC (Bachem®, I-1400). The rate of hydrolysis was kinetically measured using a SpectraMax® GeminiEM® fluorescence plate reader from Molecular Devices at an excitation wavelength of 380 nm and an emission wavelength of 460 nm. The hK6 double-mutant used in the present study had a K_m of 302 μM. Using a substrate concentration of 400 μM, the IC$_{50}$ value of an inhibitor was determined by fitting initial reaction rates over a range of inhibitor concentration to a sigmoid curve.

One cluster of confirmed actives is N-(4-aminomethyl-phenyl)-2-hydroxy-benzamide analogs as shown in Table 1. As demonstrated by the structure–activity relationship (SAR), the amino

group of the benzylamine is required for the hK6 activity. Alkylation at the amino nitrogen, as well as substitutions alpha to the nitrogen, renders the compound inactive. While the number of analogs are not enough to derive a complete SAR, the t-butyl substitution at the 5 position, compound **7**, is the best for hK6 activity. The hydroxyl group of the 2-hydroxy-benzamide is also required for the activity, removing the hydroxyl group or introducing substitutions at the hydroxyl position eliminates the activity in general. This SAR is consistent with the original *in silico* model used for the virtual screening, which requires that the hydroxyl group is bound in the oxyanion hole, where multiple H-bonding interactions are formed and the space is extremely limited.

The only exception to this SAR and the *in silico* model is compound **9** which has an IC$_{50}$ of 1.7 μM. Compound **9** was initially assigned the structure of **9a**, as shown in Figure 5, which has a bulky substitution at the hydroxyl position. Based on the *in silico* model, it is impossible for this compound to have a binding affinity to rationalize its IC$_{50}$. For **9a** to bind in the same binding site, the pyridine ring must rotate 180° with the pyridine nitrogen facing the oxyanion hole. Even if the pyridine nitrogen is capable of serving as an H-bonding acceptor, the position of the pyridine ring,
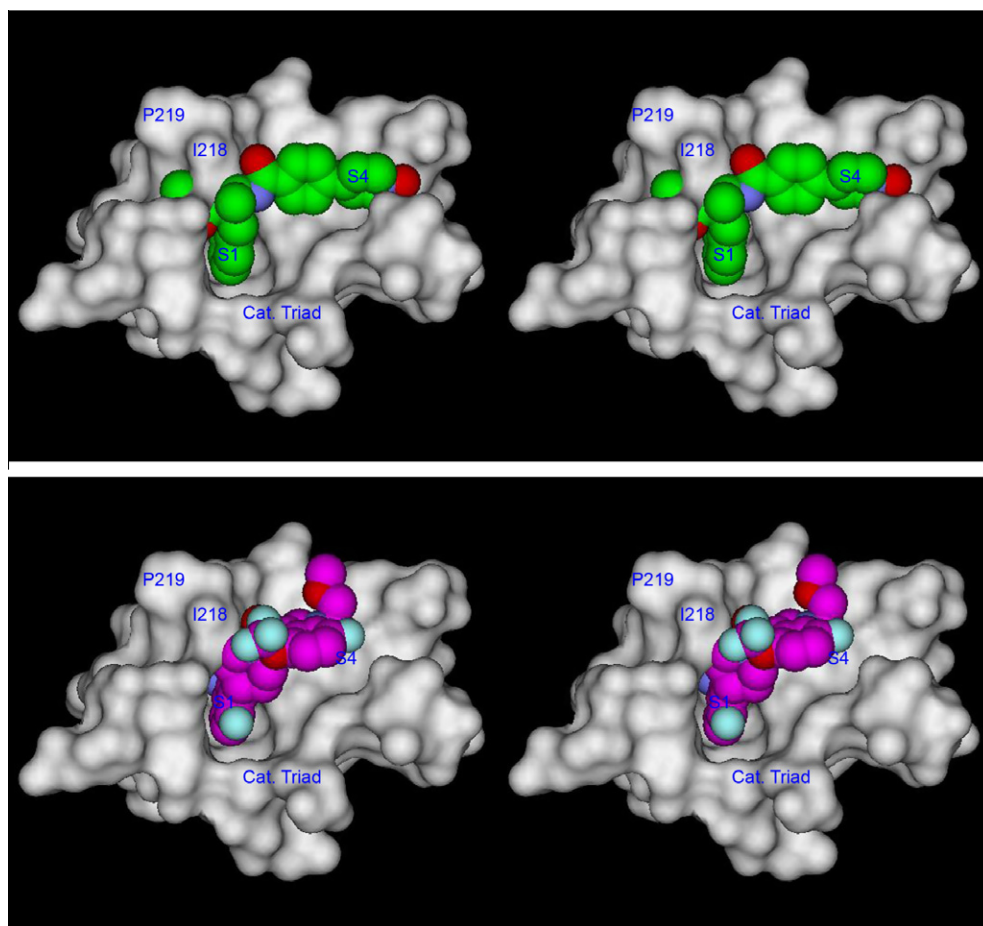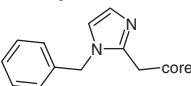
G. Liang et al. / Bioorg. Med. Chem. Lett. 22 (2012) 2450–2455

2453

Figure 4. Stereo view of fXa and β-tryptase inhibitors in a steric collision in the hK6 substrate-binding site. (Top) Otamixaban, an fXa inhibitor with its native fXa binding mode (1KSN.pdb) in hK6 substrate-binding site. Carbon atoms of Otamixaban are colored in green and those of the hK6 are colored in white. (Bottom) A β-tryptase inhibitor with its native tryptase binding mode (4A6L.pdb) in hK6 substrate-binding site. Carbon atoms of the β-tryptase inhibitor are colored in green and those of the hK6 are colored in white.

Table 1
IC$_{50}$ values of hK6 inhibitors with an amidinothiophene P1 group and a pyrrolidinone-sulphonamide scaffold linker

	X	R	IC$_{50}$ (μM)
1	C	3-Methoxy	8.6
2	C	3-Chloro	13.5
3	C	4-Chloro	7.8
4	C	4-Methoxy	20.6
5	C	4-Ethoxy	12.9
6	C	4-Dimethylamino	10.6
7	C	4-Animo	3.8
8	C	5-*t*-Butyl	0.3
9 (**9a/9b**)	N$^+$	(see Fig. 5)	1.8

Figure 5. Two possible structures, **9a** and **9b**, for the same compound registration **9**.

however, cannot properly present the nitrogen into the oxyanion hole. This inconsistency was further confirmed by a follow-up analytical investigation using both MS and NMR, which indicated that **9b** was the actual structure of compound **9**, even if both **9a** and **9b** were possible products according to the original synthetic route.
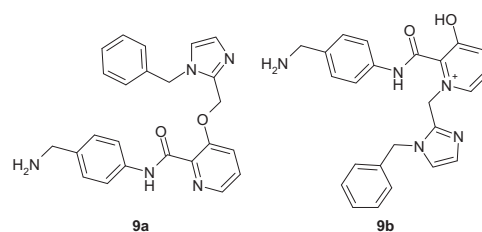
To investigate experimentally how compound **9** (**9a/9b**) binds to hK6. We conducted crystallographic studies of a complex between compound **9** and hK6. Protein used for crystallization was further purified with gel-filtration chromatography to homogeneity, and concentrated to 11.5 mg/mL. In the hanging drop crystallization, 1 μL hK6 protein stock was mixed with 1 μL well solution (Tris–HCl 0.05 M pH8.5, PEG4000 8%) containing 10 mM benzamidine. Compound **9** was soaked into hK6-benzamidine crystals.

X-ray diffraction data for hK6-compound **9** crystals were collected in-house using a Rigaku Raxis IV++ detector. The crystal structure was solved by molecular replacement using PDB entry 1LO6 as a model. Detailed crystallography and refinement data are summarized in Table 2. The coordinates of hK6-compound **9** complex

Table 2
Crystallographic statistics for KLK6 complexed with compound **9** (values in parentheses correspond to the highest-resolution shell)

Data collection	
Rigaku Raxis IV++	
Wavelength (Å)	1.54178
Space group	$P2_12_12_1$
Cell parameters (Å)	$a = 43.185$, $b = 45.950$, $c = 109.077$
Resolution (Å)	28–1.68 (1.74–1.68)
Redundancy	8.1 (3.7)
Completeness (%)	97.6 (80.2)
$I/\sigma I$	22.1 (1.52)
R_{merge} (%)	8.3 (71.4)
Refinement	
Resolution (Å)	30–1.68
No. reflections	24,849
Percentage of R_{free}	5
R_{work}/R_{free} (%)	19.9/21.0
R.M.S. deviations	
Bond lengths	0.005
Bond angles	1.0
Ramachandran plot (%)	
Preferred region	96.7

structure have been deposited with Protein Data Bank under accession code 4D8N.

The X-ray crystallographic studies confirmed that **9b** was the actual structure for compound **9**. As shown in Figure 6, the structure of the hK6 complexed with compound **9b** consists of two adjacent beta-barrels connected with several alpha helices and turns, which are highly conserved with the structure of apo-hK6 available both internally and in public domain. This structure is also highly similar to other trypsin-like serine proteases, such as fXa, fVIIa, and β-tryptase, including the catalytic triad and the rest of the substrate-binding site, which is situated at the junction of the two beta-barrels and is openly accessible.

The electron density map, as shown in Figure 7, is well defined for the inhibitor in the substrate-binding site except for the methylene between the pyridinium ring and the imidazole ring. As further detailed in Figure 8, the benzylamine group binds in the S1 pocket with the primary amine H-bonding with the side chain of Asp189. The side chain of Ile218 further contributes to the binding affinity through hydrophobic interaction with the phenyl ring of the benzylamine. The hydroxyl group of the hydroxypyridinium
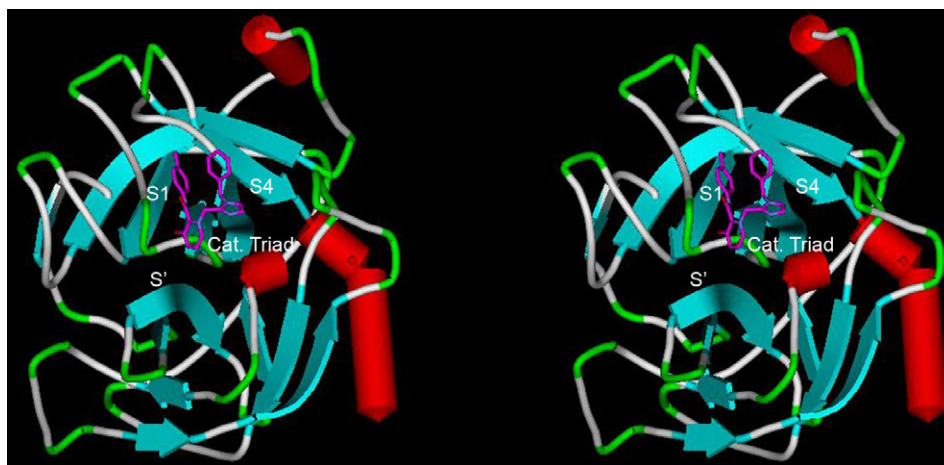

Figure 6. Stereo view of the schematic folding of hK6 complexed with compound **9b**, where the S1 pocket is occupied by benzylamine, the oxyanion hole is occupied by the pyridinol oxygen, and the aromatic tail situates closer to the S4 pocket. The coordinates of this complexed is available from Brookhaven Protein Data Bank (PDB: 4D8N.pdb).
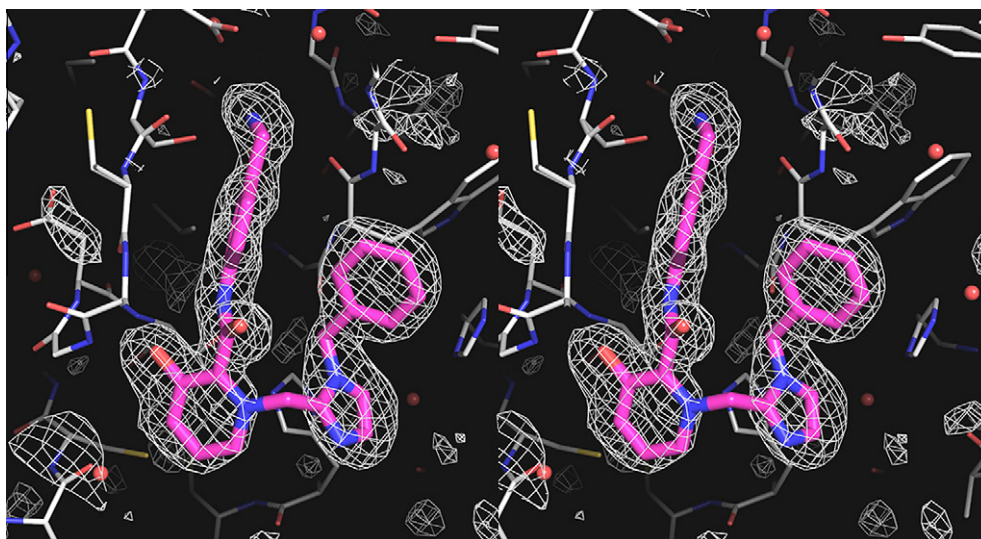

Figure 7. Stereo view of the Fo–Fc electron density (at 2σ) in the vicinity of compound **9b** before the compound was included in the model with the final model of compound **9b** superimposed. Carbon atoms of compound **9b** are colored in magenta and those of hK6 are colored in white.
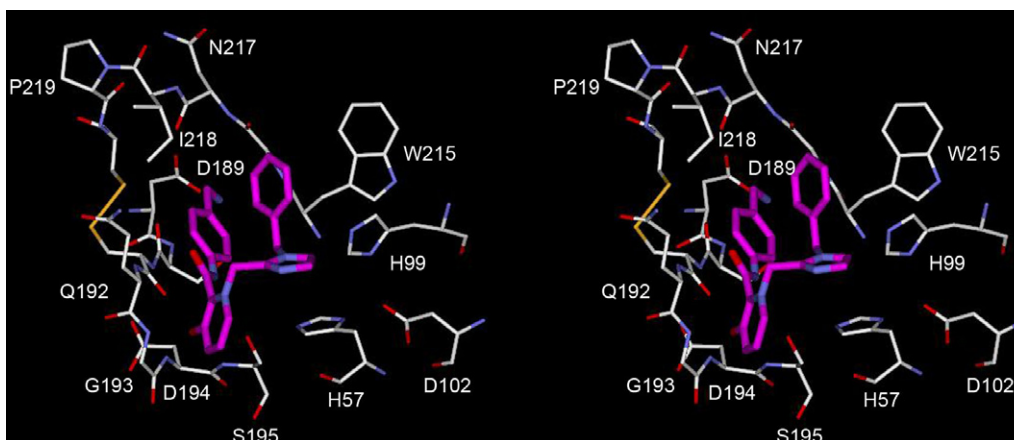
Figure 8. Stereo view of compound **9b** in hK6 substrate binding site, where carbon atoms of compound **9b** are colored in magenta and those of hK6 are colored in white.

ring, most likely deprotonated, is located in the center of the oxyanion hole, forming an H-bonding network with the backbone NH groups of Gly193 and Ser195. This part of the structure is well resolved without any ambiguity, which reconfirms the *in silico* model discussed before. The imidazole ring of **9b**, π-stacked with the side chain of His57, further projects the aromatic tail toward the S3/S4 pocket. This binding vector presents additional binding opportunities in S3 and S4 binding pockets for compound optimization.

In conclusion, a series of hK6 inhibitors with a *para*-amidobenzylamine P1 group and a 2-hydroxybenzamide scaffold linker were discovered through structure-based virtual screening with their activities confirmed through chromogenic assay. As part of the SAR deconvolution, the X-ray structure of hK6 complexed with compound **9b** was determined to a resolution of 1.68 Å. While the overall folding of the hK6 with inhibitor is highly conserved with the apo-protein, the interaction between the enzyme and the inhibitor offers further guidance for the subsequent optimization of the compound to improve both hK6 potency and selectivity against other serine proteases.

References and notes

1. Barrett, A. J.; Tolle, D. P.; Rawlings, N. D. *Biol. Chem.* **2003**, *384*, 873.
2. Yousef, G. M.; Diamandis, E. P. *Endocr. Rev.* **2001**, *22*, 184.
3. Lundwall, A.; Band, V.; Blaber, M.; Clements, J. A.; Courty, Y.; Diamandis, E. P.; Fritz, H.; Lilja, H.; Malm, J.; Maltais, L. J.; Olsson, A. Y.; Petraki, C.; Scorilas, A.; Sotiropoulou, G.; Stenman, U.-H.; Stephan, C.; Talieri, M.; Yousef, G. M. *Biol. Chem.* **2006**, *387*, 637.
4. Lundwall, A.; Brattsand, M. *Cell. Mol. Life Sci.* **2008**, *65*, 2019.
5. Chao, J. Handbook of Proteolytic Enzymes; 2nd ed.; Elsevier Academic Press, **2004**; Vol. *2*, p 1577.
6. Diamandis, E. P.; Okui, A.; Mitsui, S.; Luo, L.-Y.; Soosaipillai, A.; Grass, L.; Nakamura, T.; Howarth, D. J. C.; Yamaguchi, N. *Cancer Res.* **2002**, *62*, 295.
7. Diamandis, E. P.; Yousef, G. M.; Luo, L. Y.; Magklara, A.; Obiezu, C. V. *Trends Endocrinol. Metabol.* **2000**, *11*, 54.
8. Luo, L.-Y.; Shan, S. J. C.; Elliott, M. B.; Soosaipillai, A.; Diamandis, E. P. *Clin. Cancer Res.* **2006**, *12*, 742.
9. Oikonomopoulou, K.; Batruch, I.; Smith, C. R.; Soosaipillai, A.; Diamandis, E. P.; Hollenberg, M. D. *Biol. Chem.* **2010**, *391*, 381.
10. LeBeau, A. M.; Kostova, M.; Craik, C. S.; Denmeade, S. R. *Biol. Chem.* **2010**, *391*, 333.
11. Shaw, J. L. V.; Diamandis, E. P. *Biol. Chem.* **2008**, *389*, 1409.
12. Pampalakis, G.; Sotiropoulou, G. *Biochim. Biophys. Acta Rev. Cancer* **2007**, *1776*, 22.
13. Xi, Z.; Klokk, T. I.; Korkmaz, K.; Kurys, P.; Elbi, C.; Risberg, B.; Danielsen, H.; Loda, M.; Saatcioglu, F. *Cancer Res.* **2004**, *64*, 2365.
14. Diamandis, E. P.; Yousef, G. M.; Soosaipillai, A. R.; Grass, L.; Porter, A.; Little, S.; Sotiropoulou, G. *Clin. Biochem.* **2000**, *33*, 369.
15. Yousef, G. M.; Kishi, T.; Diamandis, E. P. *Clin. Chim. Acta* **2003**, *329*, 1.
16. Shaw, J. L. V.; Diamandis, E. P. *Clin. Chem. (Washington, DC, United States)* **2007**, *53*, 1423.
17. Blaber, S. I.; Yoon, H.; Scarisbrick, I. A.; Aparecida Juliano, M.; Blaber, M. *Biochemistry* **2007**, *46*, 5209.
18. Scarisbrick, I. A.; Blaber, S. I.; Lucchinetti, C. F.; Genain, C. P.; Blaber, M.; Rodriguez, M. *Brain* **2002**, *125*, 1283.
19. Blaber, S. I.; Ciric, B.; Christophi, G. P.; Bernett, M. J.; Blaber, M.; Rodriguez, M.; Scarisbrick, I. A. *FASEB J.* **2004**, *18*, 920.
20. Blaber, S. I.; Scarisbrick, I. A.; Bernett, M. J.; Dhanarajan, P.; Seavy, M. A.; Jin, Y.; Schwartz, M. A.; Rodriguez, M.; Blaber, M. *Biochemistry* **2002**, *41*, 1165.
21. Luo, L.-Y.; Jiang, W. *Biol. Chem.* **2006**, *387*, 813.
22. Geiger, R.; Stuckstedte, U.; Clausnitzer, B.; Fritz, H. *Hoppe Seylers Z. Physiol. Chem.* **1981**, *362*, 317.
23. Borgono, C. A.; Michael, I. P.; Shaw, J. L. V.; Luo, L.-Y.; Ghosh, M. C.; Soosaipillai, A.; Grass, L.; Katsaros, D.; Diamandis, E. P. *J. Biol. Chem.* **2007**, *282*, 2405.
24. Sealock, R. W.; Laskowski, M., Jr. *Biochemistry* **1969**, *8*, 3703.
25. Song, H. K.; Suh, S. W. *J. Mol. Biol.* **1998**, *275*, 347.
26. Koepke, J.; Ermler, U.; Warkentin, E.; Wenzl, G.; Flecker, P. *J. Mol. Biol.* **2000**, *298*, 477.
27. Lin, G.; Bode, W.; Huber, R.; Chi, C.; Engh, R. A. *Euro. J. Biochem.* **1993**, *212*, 549.
28. Kennedy, A. R. *Cancer Res.* **1999**, *1994*, 54.
29. Geratz, J. D.; Whitmore, A. C.; Cheng, M. C. F.; Piantadosi, C. *J. Med. Chem.* **1973**, *16*, 970.
30. Loeffler, L. J.; Mar, E.-C.; Geratz, J. D.; Fox, L. B. *J. Med. Chem.* **1975**, *18*, 287.
31. Geratz, J. D.; Cheng, M. C. F.; Tidwell, R. R. *J. Med. Chem.* **1975**, *18*, 477.
32. Geratz, J. D.; Cheng, M. C. F.; Tidwell, R. R. *J. Med. Chem.* **1976**, *19*, 634.
33. Okada, Y.; Tsuda, Y.; Wanaka, K.; Tada, M.; Okamoto, U.; Okamoto, S.; Hijikata-Okunomiya, A.; Bokonyi, G.; Szende, B.; Keri, G. *Bioorg. Med. Chem. Lett.* **2000**, *10*, 2217.
34. Adlington, R. M.; Baldwin, J. E.; Becker, G. W.; Chen, B.; Cheng, L.; Cooper, S. L.; Hermann, R. B.; Howe, T. J.; McCoull, W.; McNulty, A. M.; Neubauer, B. L.; Pritchard, G. J. *J. Med. Chem.* **2001**, *44*, 1491.
35. Young, W. B.; Rai, R.; Shrader, W. D.; Burgess-Henry, J.; Hu, H.; Elrod, K. C.; Sprengeler, P. A.; Katz, B. A.; Sukbuntherng, J.; Mordenti, J. *Bioorg. Med. Chem. Lett.* **2006**, *16*, 2034.
36. LeBeau, A. M.; Singh, P.; Isaacs, J. T.; Denmeade, S. R. *Chem. Biol. (Cambridge, MA, United States)* **2008**, *15*, 665.
37. LeBeau, A. M.; Banerjee, S. R.; Pomper, M. G.; Mease, R. C.; Denmeade, S. R. *Bioorg. Med. Chem.* **2009**, *17*, 4888.
38. Magklara, A.; Mellati, A. A.; Wasney, G. A.; Little, S. P.; Sotiropoulou, G.; Becker, G. W.; Diamandis, E. P. *Biochem. Biophys. Res. Commun.* **2003**, *307*, 948.
39. Bernett, M. J.; Blaber, S. I.; Scarisbrick, I. A.; Dhanarajan, P.; Thompson, S. M.; Blaber, M. *J. Biol. Chem.* **2002**, *277*, 24562.